AFOSR-TR- 88-0576

FINAL TECHNICAL REPORT

SUBMITTED TO U. S. AIR FORCE OFFICE OF SCIENTIFIC RESEARCH

Attention: Dr. Robert J. Barker
Program Manager, Physical and Geophysical Sciences
Department of the Air Force
Air Force Office of Scientific Research (AFSC)
Bolling AFB, D.C. 20332

Proposing Institution: University of Miami
Department of Physics
Coral Gables, Florida 33124

Title: Theoretical Modeling of Accelerating Arc Plasmas

Period of Final Report: 31 July 84 - 31 July 87

Principal Investigator: Dr. Manuel A. Huerta
Professor of Physics
[redacted]
Telephone No. (305) 284-2323

Signed: Manuel A. Huerta

Manuel A. Huerta
Principal Investigator
Department of Physics

Date: April 22, 1988

UNCLASSIFIED
SECURITY CLASSIFICATION OF THIS PAGE

REPORT DOCUMENTATION PAGE

1a. REPORT SECURITY CLASSIFICATION UNCLASSIFIED	1b. RESTRICTIVE MARKINGS
2a. SECURITY CLASSIFICATION AUTHORITY	3. DISTRIBUTION/AVAILABILITY OF REPORT Approved for public release; distribution is unlimited.
2b. DECLASSIFICATION/DOWNGRADING SCHEDULE	
4. PERFORMING ORGANIZATION REPORT NUMBER(S)	5. MONITORING ORGANIZATION REPORT NUMBER(S) AFOSR-TR- 88-0576
6a. NAME OF PERFORMING ORGANIZATION Univ of Miami 6b. OFFICE SYMBOL (If applicable)	7a. NAME OF MONITORING ORGANIZATION AFOSR/NP
6c. ADDRESS (City, State, and ZIP Code) P.O. Box 248293 Coral Gables, FL 33124	7b. ADDRESS (City, State, and ZIP Code) Building 410, Bolling AFB DC 20332-6448
8a. NAME OF FUNDING/SPONSORING ORGANIZATION AFOSR 8b. OFFICE SYMBOL (If applicable) NP	9. PROCUREMENT INSTRUMENT IDENTIFICATION NUMBER AFOSR-84-0116
8c. ADDRESS (City, State, and ZIP Code) Building 410, Bolling AFB DC 20332-6448	10. SOURCE OF FUNDING NUMBERS PROGRAM ELEMENT NO. 61102F; PROJECT NO. 2301; TASK NO. A6; WORK UNIT ACCESSION NO.

11. TITLE (Include Security Classification)
(U) THEORETICAL MODELING OF ACCELERATING ARC PLASMAS

12. PERSONAL AUTHOR(S)

13a. TYPE OF REPORT	13b. TIME COVERED	14. DATE OF REPORT (Year, Month, Day)	15. PAGE COUNT
FINAL	FROM 31 Jul 84 TO 31 Jul 87	22 Apr 88	31

16. SUPPLEMENTARY NOTATION

17. COSATI CODES			18. SUBJECT TERMS (Continue on reverse if necessary and identify by block number)
FIELD	GROUP	SUB-GROUP	
	20:09 19:06		

19. ABSTRACT (Continue on reverse if necessary and identify by block number)

The researchers present a calculation in a simplified geometry for the current distribution in the rails, taking into account the motion of the armature and the time variation of the current. Closed form, asymptotic, results for the current density are obtained for arbitrary time dependent currents and velocities, in the limit in which the length scale is small, where o is the electrical conductivity of the rails, and v is the speed of the armature. Because of eddy current effects the rail current may reverse in portions of the rails when the total current decreases. The current is used as a source of Joule heating to find the temperature distribution in the rails. The heat diffusivity is negligible and we are able to give numerical results concerning melting.

20. DISTRIBUTION/AVAILABILITY OF ABSTRACT ☒ UNCLASSIFIED/UNLIMITED ☐ SAME AS RPT. ☐ DTIC USERS	21. ABSTRACT SECURITY CLASSIFICATION UNCLASSIFIED
22a. NAME OF RESPONSIBLE INDIVIDUAL R J BARKER	22b. TELEPHONE (Include Area Code) (202) 767-5011 22c. OFFICE SYMBOL AFOSR/NP

DD FORM 1473, 84 MAR 83 APR edition may be used until exhausted. All other editions are obsolete.

SECURITY CLASSIFICATION OF THIS PAGE
UNCLASSIFIED

Introduction

This is a report on the work done during the third year of of this grant plus a six month no-cost extension. The project was to develop theoretical models of several aspects of accelerating arc plasmas in electromagnetic railguns with plasma driven projectiles.

The grant provided three months of support during the summer of 1986 for Dr. Huerta, and a further two months during the summer of 1987. Dr. J. C. Nearing was supported for two months during the summer of 1986. The other person who received support was Mr. G. Christopher Boynton who is a graduate student doing his dissertation on this work. He was supported fully during the whole year and a half.

A group of researchers on railgun problems was developed at the University of Miami largely due to the support flowing from this project. There appeared a strong possibility of funding by the SDIO(IST) office of a consortium proposed by Dr. Huerta, Dr. Harry S. Robertson, and other faculty at the University of Miami. Several of us attended the 23 June 1986 EML Science Interchange Workshop at the Air Force Armament Laboratory of Eglin Air Force Base that was sponsored by Dr. Leonard Caveny of SDIO(IST). There I presented our research plans on fundamental processes in rapidly moving high current arcs. Soon thereafter we received two letters of intent to fund. Delays kept coming up, however. Col David Finkleman asked us several times to submit extensively revised proposals following SDIO/IST instructions. I made a presentation to Drs. Dwight Dustin and Caveny, at SDIO(ISDT) headquarters in Washington in February, 1987. Finally our proposal was declined declined in April of 1987. A great deal of time and energy was wasted by the P. I. and others during this process. The whole episode was a fiasco.

Description of the Technical Work

During the second year of this project Miss Ann Decker obtained her Ph. D. submitting a dissertation on the effects of finite conductivity and compressibility on the development of the Kruskal-Schwarzchild instability. The inclusion of finite conductivity effects produced a fourth order eigenvalue equation for the modes. She did a numerical solution of the equation and obtained a dispersion relation. Part of that work was presented by the P. I. at the First EM Gun Armature Workshop, 24-26 June, 1986. In the course of preparing this work for publication the P. I. found that Miss Decker had neglected to examine the effects of a singularity in the fourth derivative term of the mode equation. This has called for a revision of the problem. A physicist on a sabbatical visit from Argentina, Dr. Felix Rodriguez-Trelles, has been of great help in this.

The work with Dr. Nearing concentrated on modeling the current in the rails for arbitrarily time dependent current and velocity. Also the temperature distribution was obtained in important cases. A paper on this work was submitted for the 4th Symposium on Electromagnetic Launch Technology in Austin Texas during April 11-14 1988, and for publication in the IEEE Transactions on Magnetics. A copy of this paper is attached.

The work with Mr. Boynton centers on a two dimensional time dependent simulation of plasma armatures. We use the equations of resistive MHD and we use a two dimensional FCT code to advance all quantities in time. A good deal of effort has also expended on developing graphical methods that allow good display of the results. We have done several runs in the University of Miami's VAX 8650, which does about 1,000 steps per hour of

CPU time. A paper with some of the results of this work for an adiabatic case was also submitted for the 4th Symposium on Electromagnetic Launch Technology in Austin Texas, and for publication in the IEEE Transactions on Magnetics. A copy of this paper also is attached. We have results beyond those prepared for the Austin conference. The last figures attached represent the pressure in the plasma developing in time from 120,000 time steps, 87μsec since firing, with the armature 4.6 cm down the barrel, in five figures until the last one at 89.87μsec with a travel of 4.9 cm. The plasma was initially in mechanical equilibrium with a 2% perturbation of the pressure near the rear of the armature. By the time the armature has advanced only about 5 cm serious disruptions appear in it. Due to the violent plasma motions the time step has to be reduced as we go along to satisfy the Courant condition and prevent crashes due to numerical instabilities. This is having a bad effect on the CPU time requirement.

Clearly this problem is one that requires a supercomputer. During the summer of 1988 Dr. Huerta and Mr. Boynton are going to be working at Eglin AFB under the USAF Summer Faculty Research Program. We expect to be able to use the Cyber 205 at AFATL. This would be of great benefit to our research.

SKIN AND HEATING EFFECTS OF RAILGUN CURRENT

J. C. Nearing and M. A. Huerta
University of Miami
Physics Department
Coral Gables, FL 33124

Abstract

We present a calculation in a simplified geometry for the current distribution in the rails, taking into account the motion of the armature and the time variation of the current. Closed form, asymptotic, results for the current density are obtained for arbitrary time dependent currents and velocities, in the limit in which the length scale k_0^{-1} is small, where $k_0 = (\mu_0 \sigma v)$. σ is the electrical conductivity of the rails, and v is the speed of the armature. Because of eddy current effects the rail current may reverse in portions of the rails when the total current decreases. The current is used as a source of Joule heating to find the temperature distribution in the rails. The heat diffusivity is negligible and we are able to give numerical results concerning melting.*

Introduction

In a railgun the current goes into one rail, passes through the armature, and returns via the other rail. The armature is immersed in the magnetic field produced by the rail currents and experiences a strong magnetic force that pushes the projectile in front of it. The distribution of current in the rails is one of the important factors in the operation of railguns because it determines the rail resistance and the joule heating losses. A great deal of work has been done to model this current distribution. Kerrisk[1,2] did a numerical calculation of the current distribution and of the accompanying temperature distribution, allowing the electrical conductivity to depend on temperature and the magnetic permeability to depend on magnetic field strength. He treated carefully the two dimensional variations in the rectangular cross section of the rails but neglected the variations in the direction along the rails. Marshall[3] discussed qualitatively the problem of the variation along the rails. Long[4] attempted a solution for a case with steady current and speed. Drake and Rathmann[5] obtained infinite series solutions that described the variation of the skin depth along the rail due to the motion of the armature.

In a railgun, the part of the rails ahead of the armature is in a region where there is almost no magnetic field. As the armature sweeps along the rails, the rails are exposed to the strong field behind the armature. Due to the rapid motion of the armature along the rails, the current and magnetic field do not have time to diffuse completely into the rails and are concentrated in a skin layer near the rail surfaces. We seek to describe analytically how the magnetic field and current diffuse into the rails and what the temperature distribution caused by the Joule heating is. The important skin depth that arises can be written as $\delta = \sqrt{4t/\mu_0 \sigma}$, where t is the time since the magnetic field started to diffuse into the conductor of conductivity σ, and magnetic permeability μ_0. There are several related problems presented by Knoepfel[6] with known analytic solutions.

* This work supported in part by the Air Force Office of Scientific Research under grant number 84-0116.

They involve the calculation of the magnetic field and current inside a semi-infinite space bounded by a plane, or inside a cylinder, when the magnetic field outside is uniform in space and has a known time dependence.

In order to elucidate the effects of the motion of the armature, our analytic solution takes into account the variations along the rail direction, x as shown in Fig. 1. The rails

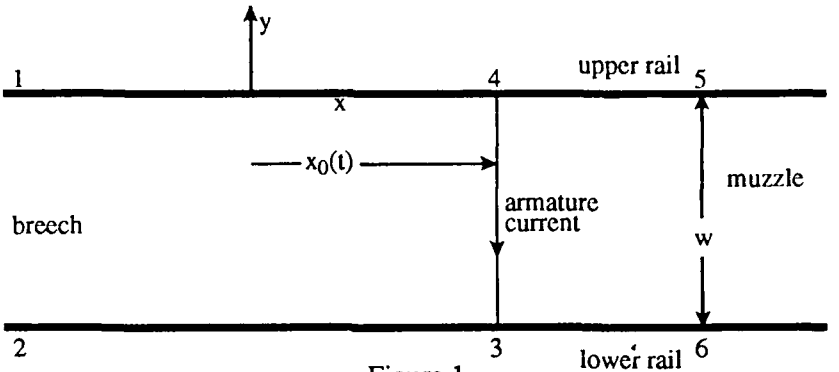

Figure 1

are taken as infinitely thick because their thickness is much greater than the skin depth. We also take into account variations in the current density in the direction into the rails, y. This will enable us to describe skin depth effects on the inside surface of the rails. We simplify the geometry by neglecting variations in the z direction, in effect making the problem that of two rails of infinite height. In a complete treatment of the problem $J_y(t)$ in the armature would be determined by the properties of the armature in conjunction with the properties of the rails. We model the armature by an assumed time dependent distribution of current density in an armature moving to the right along the rails with an arbitrary velocity $v_0(t) = dx_0/dt$.

We obtain rigorous general results for the current distribution in the rails and find the temperature distribution for special cases. We get conditions for melting depending on the current, and much less strongly on the length of the arc. We also give an expression for the breech voltage in terms of the current, and discuss the circumstances when it reduces to the simple expressions that are typically used in railgun circuit models. One of the most interesting results is the reversal of current density in the rails, and possibly in the armature, whenever the total rail current decreases.

Current Calculation

In the coordinate system shown in Fig. 1, the upper rail occupies the space $y > 0$. The numbers 1–6 are used later to identify important voltages. The lower rail occupies the space $y < -w$ and carries a current that is a mirror image of the current in the upper rail. The armature between the rails occupies the space $-w < y < 0$ and has a current density $J_y(x,t)$

$$J_y(x,t) = -I'(t)f(x - x_0(t))$$

where I' is the current per rail height, f represents the spatial distribution of the current in the armature, and $x_0(t)$ is the position of the center of the armature. f is normalized

to $\int f(x)dx = 1$. Everything is independent of z, and only the x, y, and t dependencies are to be determined. To analyze the fields resulting from this source, we write J_y as a Fourier integral

$$J_y(x,t) = \int \frac{dk}{2\pi} \int \frac{d\omega}{2\pi}\, g(k)h(k,\omega)e^{i(kx-\omega t)}\ , \quad (-w < y < 0) \tag{1}$$

$$f(x) = \int \frac{dk}{2\pi}\, g(k)e^{ikx}, \qquad h(k,\omega) = -\int dt\, I'(t)e^{-ikx_0(t)}e^{i\omega t}.$$

In Maxwell's equations we neglect the displacement current compared to the conduction current because all the time constants considered are much larger than ϵ_o/σ. The resulting equations are

$$\nabla \times \mathbf{B} = \mu_0 \mathbf{J} \qquad \text{and} \qquad \nabla \times \mathbf{E} = -\frac{\partial \mathbf{B}}{\partial t}\ .$$

In the domain $y < 0$, a vacuum, the magnetic field due to a current density $J_y = e^{i(kx-\omega t)}$ is

$$B_z = \frac{i\mu_0}{k}\, e^{i(kx-\omega t)} \qquad (y < 0).$$

Taking the full J_y of Eq. (1) into account we find the magnetic field for $y < 0$ to be

$$B(x,y,t) = -\mu_0 I'(t) \int_{\xi}^{\infty} dx'\, f(x') \qquad (y < 0), \tag{2}$$

where $\xi = x - x_0(t)$. The absolute value $|\xi|$ is the distance along the rail from the point with coordinate x to the center of the armature. In arriving at (2) we have used the integral

$$\frac{i}{2\pi} \int_{-\infty}^{+\infty} \frac{dk}{k} e^{ikx} = \begin{cases} 1 & x < 0 \\ 0 & x > 0 \end{cases}$$

where the path of integration goes above the pole at $k = 0$. The magnetic field of Eq. (2) is constant behind the armature, where $\xi < 0$, and zero ahead of it, where $\xi > 0$, as one would expect in this geometry.

In the domain $y > 0$, the interior of the upper rail, the electric field is eliminated using the conductivity equation, $\mathbf{J} = \sigma \mathbf{E}$. Eliminating $\mathbf{E}$ and $\mathbf{J}$ from Maxwell's equations gives the diffusion equation for the magnetic field

$$\nabla^2 \mathbf{B} = \mu_0 \sigma \frac{\partial \mathbf{B}}{\partial t}\ . \tag{3}$$

The vector $\mathbf{B}$ has only a z-component. A single Fourier component is written $B_z = F(y) \exp\left[i(kx - \omega t)\right] \quad (y > 0)$. When this is substituted in Eq. (3), the resulting equation is

$$\partial_y^2 F + (i\omega\sigma\mu_0 - k^2)F = 0,$$

whose solution is

$$F(y) = \frac{i\mu_0}{k}\, e^{\alpha y}, \qquad \alpha = \sqrt{k^2 - i\mu_0\sigma\omega}. \tag{4}$$

The coefficient for $F(y)$ comes from the continuity of B_z at $y = 0$.

Since the fields and currents must die off as y becomes large and positive, the sign of the square root is $\Re(\alpha) < 0$. In order to obtain the value of the magnetic field for $y > 0$, we integrate over k and ω in Eq. (1). The value of B for $y > 0$ will then be

$$B_z(x,y,t) = -i\mu_0 \int dt' \int \frac{dk}{2\pi} \int \frac{d\omega}{2\pi}\, \frac{1}{k} \cdot I'(t') g(k) e^{\alpha y + i(kx - \omega t)} e^{-i(kx_0(t') - \omega t')}\,. \tag{5}$$

The ω integral can be done with no further assumptions on the time dependence of I', or the shape f of the armature's current distribution. The integral $\int e^{\alpha y - i\omega(t-t')} d\omega/2\pi$ is zero for $t < t'$. The integrand has a branch point at $\omega = -ik^2/\mu_0\sigma$, so when $t > t'$, we deform the contour around this branch toward $-i\infty$. Change variables to $s = i\omega - k^2/\mu_0\sigma$ and observe that the imaginary part of the integral vanishes. Using integration by parts we obtain

$$B_z = -i\mu_0 \int_{-\infty}^{t} dt'\, I'(t') \int \frac{dk}{2\pi}\, \frac{1}{k} g(k) e^{ik(x - x_0(t'))} \cdot \frac{y}{2}\sqrt{\frac{\sigma\mu_0}{\pi(t-t')^3}}\, e^{-k^2(t-t')/\mu_0\sigma} e^{-y^2\mu_0\sigma/4(t-t')}\,, y > 0. \tag{6}$$

The integral of Eq. (6) is a general expression for the magnetic field in this geometry. (The behavior of this expression as $y \to 0$ needs to be treated carefully.) In order to make further progress on this integral, it is necessary to assume a shape for the current distribution in the armature. We have considered several forms for $f(x)$. One of the simplest forms to take that yields interesting results is

$$f(x) = \frac{1}{2L} \quad (-L < x < L).$$

With this form, the k integral of Eq. (6) can be done. It is of the form

$$\int \frac{dk}{2\pi}\, \frac{1}{k}\, \frac{\sin kL}{kL} e^{ikx - \alpha k^2}.$$

The contour goes from $-\infty$ to $+\infty$, passing above the singularity at $k = 0$. Bring the contour down to the real-k axis, and we get a principal value integral plus a semi-circular contour just over the pole at zero. Only the cosine part of $\exp(ikx)$ contributes to the latter, and only the sine part to the former. This integral is then

$$-\frac{i}{2} + \frac{i}{\pi} \int_0^{\infty} dk \frac{\sin kL}{kL} \frac{\sin kx}{kx} e^{-\alpha k^2}.$$

We combine the two sines into the difference of cosines and use a tabulated[7] integral to obtain

$$B_z(x,y,t) = -\mu_0 y\sqrt{\frac{\mu_0\sigma}{16\pi}}\int_{-\infty}^{t} dt' I'(t')(t-t')^{-3/2}\ e^{-y^2\mu_0\sigma/4(t-t')}$$
$$\cdot\Bigg\{1+\frac{1}{2L}\Bigg[(x-x_0-L)\,\mathrm{erf}\left[(x-x_0-L)\sqrt{\mu_0\sigma/4(t-t')}\right]$$
$$-(x-x_0+L)\,\mathrm{erf}\left[(x-x_0+L)\sqrt{\mu_0\sigma/4(t-t')}\right]$$
$$+2\sqrt{\frac{t-t'}{\pi\mu_0\sigma}}\Big[e^{-(x-x_0+L)^2\mu_0\sigma/4(t-t')}$$
$$-e^{-(x-x_0-L)^2\mu_0\sigma/4(t-t')}\Big]\Bigg]\Bigg\}. \tag{7}$$

The above expression for the magnetic field allows an arbitrary thickness L for the armature, an arbitrary time dependence for the current $I(t)$, and a general time dependence for the armature position $x_0(t)$. The curl of this expression for B_z will give the current density. Rather than writing down the complicated expressions that result in the general case, we will specialize to two cases of interest. In the first case we consider a thin armature ($L \to 0$) with a general time dependent current and velocity. The thin armature case simplifies the derivation of an approximate current–voltage relation for the railgun. It also allows a closed form analytical expression for the temperature rise caused by very concentrated currents. In the second case we will consider a thick armature but with the current and the velocity kept constant in time. This case is of interest because we are able to calculate the temperature rise of the rails for realistically large arcs.

Time dependent results for a thin armature

A thin armature could represent the sort of current spots ,or filaments, that are observed. In this section, then, $I'(t)$ could represent the current in a spot, and not the total current through the rail. Of course, due to the two dimensional nature of our model, the spot is really modeled as a sheet. The thin armature result is obtained by taking the limit as $L \to 0$ in Eq. (7)

$$B_z(x,y,t) = -\mu_0 y\sqrt{\frac{\mu_0\sigma}{16\pi}}\int_{-\infty}^{t} dt'\, I'(t')(t-t')^{-3/2} \tag{8}$$
$$\cdot\, e^{-y^2\mu_0\sigma/4(t-t')}\left[1-\mathrm{erf}\left[(x-x_0(t'))\sqrt{\mu_0\sigma/4(t-t')}\right]\right].$$

The curl of this expression for B_z will give the current density $\mathbf{J}$. The singularity as $y \to 0$ is best treated by rewriting B_z as

$$B_z(x,y,t) = \frac{-\mu_0}{\sqrt{\pi}}\int_0^{\infty} ds\, e^{-s^2} I'(t')\left[1-\mathrm{erf}\left[\frac{s}{y}(x-x_0(t'))\right]\right], \tag{9}$$

where $t' = t - y^2\mu_0\sigma/4s^2$. The form of (9) is well behaved as $y \to 0$. The current is

$$J_x(x,y,t) = -\frac{2}{\pi}\int_0^\infty dk\, e^{-k^2y^2} I'(\tau)e^{-u^2}\left[u - \frac{\mu_0\sigma}{2k}\frac{dx_0(\tau)}{d\tau}\right] + \frac{1}{\sqrt{\pi}}\int_0^\infty dk\, e^{-k^2y^2}\frac{\mu_0\sigma}{2k^2}\left[1-\mathrm{erf}(u)\right]\frac{dI'(\tau)}{d\tau}, \tag{10}$$

and

$$J_y(x.y,t) = -\frac{2}{\pi}y\int_0^\infty dk\, ke^{-k^2y^2} I'(\tau)e^{-u^2}, \tag{11}$$

where $u = k\left[x - x_0(\tau)\right]$, and $\tau = t - \mu_0\sigma/4k^2$. The simplest special case is where the current is constant, $I'(t) = I'$, and the velocity of the thin armature is also constant, $x_0(t) = vt$. The above integrals for the current can then be evaluated in closed form throughout the rails,

$$J_x = \frac{I'k_0}{2\pi}e^{-k_0\xi/2}\left[K_0(k_0r/2) - \frac{\xi}{r}K_1(k_0r/2)\right], \tag{12}$$

and

$$J_y = -\frac{I'k_0}{2\pi}\frac{y}{r}e^{-k_0\xi/2}K_1(k_0r/2), \tag{13}$$

where $k_0 = \mu_0\sigma v$ is an inverse length that can be used to scale all of the variables, $r = \sqrt{\xi^2 + y^2}$ is the distance from the field point to the present position of the armature, ξ was defined below (2), and the K's are Bessel functions of the second kind with imaginary argument. At a distance from the current source large compared to k_0^{-1}, the current density of Eqs. (12) and (13) has the asymptotic form[8]

$$\mathbf{J} \sim \frac{I'k_0}{2\pi}\sqrt{\frac{\pi}{k_0r}}e^{-k_0(\xi+r)/2}\left[\left(1-\frac{\xi}{r}\right)\hat{\mathbf{x}} - \frac{y}{r}\hat{\mathbf{y}}\right]. \tag{14}$$

From here one can show that the shape of these flow lines is parabolic at large distances from the origin. In Eq. (14) the space in front of the armature has $\xi > 0$ and $r > 0$ so the exponential is damped very quickly (for large k_0) giving negligible current ahead of the armature as expected. Behind the armature, $\xi < 0$, there is damping for $y > 0$, but along the rail surface the exponent is zero.

The current of Eqs. (10) and (11) can be evaluated asymptotically for a general armature current and velocity. The integrals are approximated using the method of steepest descent; We have done this calculation. It is straightforward but somewhat long. In the region where $x_0(t) - x \gg y > 0$ there is a much simpler way to obtain the current. For large σ the argument of the error function in Eq. (9) varies rapidly. We make the approximation that the error function is a step function, with $1 - \mathrm{erf}(x) \approx 2$ for $x < 0$, and $1 - \mathrm{erf}(x) \approx 0$ for $x > 0$. Then the magnetic field of Eq. (9), behind the armature where $\xi = x - x_0(t) < 0$, is approximately

$$B_x(x,y,t) \approx -\frac{2\mu_0}{\sqrt{\pi}}\int_{s_w}^\infty ds\, e^{-s^2} I'\left(t - \sigma\mu_0 y^2/4s^2\right), \tag{15}$$

with $s_x = y/\delta$, and we have introduced a skin depth δ defined by

$$\delta = \sqrt{\frac{4(t - t_x)}{\mu_0 \sigma}}, \tag{16}$$

where $t_x < t$ is the time when the armature passes position x, defined by $x_0(t_x) = x$. Eq. (15) has a pleasing form and is similar to some of the results in Knoepfel.[6] We obtain the currents from the curl of Eq. (15),

$$J_x(x,y,t) \approx \frac{2}{\delta\sqrt{\pi}} \left[I'(t) e^{-y^2/\delta^2} \right. \tag{17}$$
$$\left. + \int_{t_x}^{t} dt' \, \frac{dI'}{dt'} \left[\sqrt{\frac{t - t_x}{t - t'}} e^{-\mu_0 \sigma y^2/4(t-t')} - e^{-y^2/\delta^2} \right] \right],$$

and

$$J_y(x,y,t) \approx \frac{-1}{\delta\sqrt{\pi}} \frac{y}{v_x(t - t_x)} I'(t_x) e^{-y^2/\delta^2}, \tag{18}$$

where v_x is the velocity at time t_x. We have written J_x in Eq. (17) so that the first term contains $I'(t)$. If that term is combined with the second term in the integral it can be seen that the first term would then contains $I'(t_x)$. We note that even if $I'(t)$ remains positive, $J_x(x,y,t)$ may become negative because of the term with dI'/dt, whenever the current decreases. Eqs. (17) and (18) are very accurate when we are just a few lengths $(\mu_0 \sigma v)^{-1}$ away from the present position of the armature. This was verified by extensive comparisons with numerical evaluations of the exact expressions in Eqs. (10) and (11).

The length k_0^{-1} is very small in typical rail launcher situations. For the case of copper at room temperature, and a speed of 1 km/sec, the length $k_0^{-1} = 1.25 \times 10^{-5}$ meters.

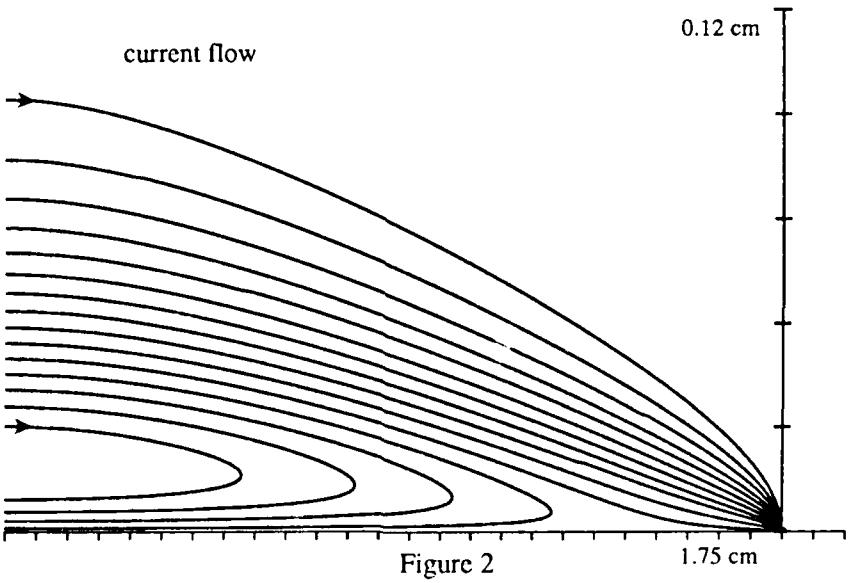

Figure 2

A picture of the current flow for these parameters is shown in Fig. 2. The acceleration is 8×10^7 m/s^2. Here the lines are tangent to the current density vector $\mathbf{J}$ and the curves are drawn at equal increments of current; the last curve includes 95% of the total current. The current has passed its peak and is decreasing. Some reverse current flow is evident in the graph in regions where $J_x(x,y,t)$ has become negative. This should not be surprising. This reverse current is just an eddy current that is trying to keep the magnetic field in the rail from dropping in value as the total rail current decreases. The total horizontal scale is 1.75 cm; the total vertical scale is expanded to 0.12 cm.

Breech and Muzzle Voltages

There are several circuit models[7,8] used to describe rail launchers as circuit elements; these require expressions for the voltages in terms of the currents. These expressions can be obtained by application of the theorem

$$\frac{d}{dt}\int \mathbf{B}\cdot d\mathbf{S} = \int \left[\frac{\partial \mathbf{B}}{\partial t} - \nabla\times(\mathbf{u}\times\mathbf{B}) + (\nabla\cdot\mathbf{B})\mathbf{u}\right]\cdot d\mathbf{S},$$

where the surface integral is taken over a surface moving with local velocity $\mathbf{u}$. For the magnetic field $\mathbf{B}$, using Maxwell's equations, we obtain

$$\frac{d}{dt}\int \mathbf{B}\cdot d\mathbf{S} = -\oint [\mathbf{E}+\mathbf{u}\times\mathbf{B}]\cdot d\mathbf{r}, \tag{19}$$

where the closed line integral is taken over the moving path. In a moving conductor Ohm's law is $\mathbf{J} = \sigma(\mathbf{E}+\mathbf{u}\times\mathbf{B})$.

For simplicity we will derive the circuit equations using the thin armature results. Integrating Eq. (19) around the path 3-4-5-6 shown ahead of the armature in Fig. 1, we find that the muzzle voltage V_m is

$$V_5 - V_6 = V_m(t) = V_a(t) = \int_{-w}^{0} \frac{J_a(t)}{\sigma_a} dy_{34}, \tag{20}$$

where J_a and σ_a are the current and conductivity of the armature, w is the rail separation, and V_a is the resistive voltage drop across the armature. We have used the fact that $\mathbf{B}$ is zero ahead of the armature in this simple geometry and that the current is extremely small ahead of the armature. This is why the muzzle voltage in Eq. (20) is given by just the resistive drop in the armature.

We use the path of integration 1-2-3-4 shown behind the armature in Fig. 1 to find that the breech voltage V_b is

$$\begin{aligned} V_b(t) &= V_2 - V_1 \\ &= \frac{d}{dt}\big(B(t)wx_0(t)\big) + 2\int_0^{x_0(t)} \frac{J_x(t)}{\sigma} dx_{14} + V_a(t), \end{aligned} \tag{21}$$

where $x_0(t)$ is the position of the armature at time t. Here we have used the fact that in this geometry B_z is uniform behind the armature and that the integral $2 \rightarrow 3$ is the same as the integral $4 \rightarrow 1$.

The breech voltage $V_b(t)$ involves the integral of J_x along the rail's inner edge, $y = 0$. Equation (17) shows that $V_b(t)$ does not depend on only the values of I' and dI'/dt at time t, but on their time history. The circuit equation will therefore be an integro-differential equation. If dI'/dt' in the integral is not too large, as is the case in most rail launchers, we can simplify the result by doing a Taylor expansion around the upper limit of integration and carrying out the t' integral. The result is

$$J_x(x,0,t) \approx \frac{2}{\delta\sqrt{\pi}} I'(t) + \frac{\mu_0\sigma\delta}{2\sqrt{\pi}} \left[\frac{dI'(t)}{dt} - \frac{1}{6}(t-t_x)\frac{d^2I'}{dt^2} + \frac{1}{30}(t-t_x)^2\frac{d^3I'}{dt^3} + \cdots \right] \tag{22}$$

which is an expansion in powers of $(t - t_x)$. Especially nearer the armature, the contributions of the higher derivatives of I' in Eq. (22) may be neglected compared to the first derivative. We can now use these results in writing the breech voltage of Eq. (21). We use the fact that behind the armature, between the rails,

$$B(x,0,t) = \mu_0 I(t)/h,$$

where h is the rail height, and I(t) is the total rail current, $I(t) = hI'(t)$, to write

$$V_b(t) \approx \frac{d}{dt}\left[\mu_0 \frac{w}{h} x_0(t) I(t)\right] + I(t)\frac{4}{h\sqrt{\pi}} \int_0^{x_0} \frac{dx}{\sigma\delta} + V_a(t) + \mu_0 \frac{1}{h\sqrt{\pi}} \frac{dI}{dt} \int_0^{x_0} \delta\, dx + \cdots \tag{23}$$

The first term in $V_b(t)$ allows us in this simple geometry to calculate the usual rail inductance

$$L_0(t) \approx \mu_0 \frac{w}{h} x_0(t) \tag{24}$$

proportional to the distance x that the armature has traveled. The second term is the rail resistance term. The skin depth that enters there involves the time $t - t_x$, which is the time since the armature passed position x. The term $V_a(t)$ is the resistive drop in the armature. The last derivative term in Eq. (23) is a skin inductance term that is small compared to the main inductance in typical railgun situations. The ellipsis indicate the presence of second and higher derivatives from Eq. (22). These would be negligible only for slowly varying currents.

The effective resistance of each rail can be read from Eqs. (16) and (23). We use the definitions of t_x and δ to write the rail resistance at time t as

$$R(t) = \frac{1}{h}\sqrt{\frac{\mu_0}{\pi\sigma}} \int_0^t dt' \, \frac{v_0(t')}{\sqrt{t-t'}}, \tag{25}$$

where $v_0(t) = dx_0(t)/dt$. $R(t)$ can be expressed in terms of the instantaneous armature position x only if x is known as a function of t. We note that an elementary derivation of $R(t)$ would miss the $\sqrt{\pi}$ factor. For example if the armature speed is constant we get

$$R(x) = \frac{2}{h\sigma}\sqrt{xv\mu_0\sigma/\pi} \tag{26}$$

where we used $x = v_0 t$. This implies that there is no fixed resistance per length, but rather that the resistance varies more slowly with length than linearly. The case of constant acceleration, $x = at^2/2$ gives

$$R(x) = \frac{4}{3h}\sqrt{\frac{\mu_0}{\sigma\pi}}a^{1/4}(2x)^{3/4}.$$

Temperature Distribution

The local heating of the rail is proportional to the square of the current density. Solve the heat diffusion equation

$$\rho c\frac{\partial T}{\partial t} - K\nabla^2 T = \frac{J^2}{\sigma},$$

neglecting the latent heat of melting, where c is the specific heat per mass, ρ is the mass density, K is the heat conductivity, and T is the temperature. The general solution of this equation in our geometry can be given in terms of Green's functions. We only need however, the case of small dimensionless diffusion coefficient, $D = K\mu_0\sigma/\rho c \ll 1$. ($D = 0.0053$ for copper at room temperature.) In this case one can verify that the the heat diffusion is negligible. During the short time that the current flows, the heat generated at a point in the rails, $\int dt\, J^2/\sigma$, does not have time to diffuse away but rather it stays where it is produced. The temperature rise at a point is then

$$T(x,y,t) = \frac{1}{\rho\sigma c}\int^t dt'\, J^2(x,y,t') \tag{27}$$

This formula implies that the rate of heating is greater at points near the arc, but it also says that the higher temperatures are reached at points farther behind the arc (closer to the breech). This happens because the heat diffusion in this short time is so small, and because points near the breech are subjected to the current for a longer time. Of course radiation cooling can affect this.

First we will calculate the temperature at the rail surface for the case of a thick armature of length $2L$. The special case where both the rail current and the velocity are constant in time allows us to express the current *at* the rail surface in closed form. Due to the lack of heat diffusion this will be the most important part of the current needed to understand the ohmic heating and melting of the surface. The y-component of the surface current density is zero except in the armature region from $\xi = -L$ to $\xi = +L$, where it has the value $I'/2L$. Recall that $|\xi|$ is the distance along the rail from the point with coordinate x to the center of the armature. The x-component of the current density at the $y = 0$ rail surface is given by

$$J_x(x,0,t) = \frac{I'}{2\pi L}\Big[M\big(k_0(\xi+L)\big) - M\big(k_0(\xi-L)\big)\Big] \tag{28}$$

where $$M(x) = \big[(x+1)K_0(|x|/2) - |x|K_1(|x|/2)\big]e^{-x/2}\ .$$

The temperature at the surface can be found in the approximation of Eq. (27) using the current of Eq. (28). The integral is readily evaluated numerically. The temperature is $\mu_0 I'^2/\rho c$ times a dimensionless factor depending on $k_0 L$ and $k_0 \xi$. For $k_0 L = 25$ and $k_0 \xi = -50000$, the factor is 3.04; for $k_0 L = 25$ and $k_0 \xi = -5000$ the factor is 2.31. For $k_0 L = 2000$ and the same ξ's, the factors are 1.63 and 0.89 respectively.

Again we take copper at room temperature and a speed of 1 km/sec, where the scaling factor $k_0 = 8 \times 10^4$ m^{-1}, so a $k_0 \xi$ of 50000 becomes 0.63 m; $k_0 L = 25$ gives an armature width $2L$ of 0.6 mm; $k_0 L = 2000$ corresponds to the width $2L$ of 5 cm. Using the room temperature values of ρ and c, and a typical value of the current density 3×10^7 Amp/meter, the factor 3.04 gives a temperature rise of 985 C. The factor 1.63 gives 528 C. The melting point of copper is 1083 C so these examples do not lead to melting.

The temperature rise is far less sensitive to the length of the arc than it is to the overall current per height of the rail. This is essentially because the penetration of the current into the rail is small for a long time; so, even if the length of the arc is long, all of the current will eventually have to pass near any given part of the surface. That the current does gradually move into the rail is reflected in the weak sensitivity of the temperature to the arc length. A factor of 80 in $k_0 L$ causes a factor of less than 2 in the final temperature. The weak sensitivity to the armature length L and the strong I'^2 dependence implies that the arc height is more important than the arc length in raising the temperature. Local pinching of the arc and concentration of the current can then give local melting. In the examples of the previous paragraph, the copper will reach its melting point at 0.63 m away from a 6 mm wide armature if the current is increased by 5%. In the case of the 5 cm long armature, a 40% change in current will be required.

The thin armature results can be used to model lateral pinching of the arc into a sheet of current. In reality current filaments form spots, not sheets of current. However, many filaments moving together, as are sometimes observed, might be approximated by a sheet. We calculate the temperature rise in the case of the thin armature with constant current and velocity. Remarkably simple analytic results will be obtained. We substitute the asymptotic form of the current in Eq. (15) into Eq. (28) and obtain

$$T(x,y,t) \approx \frac{I_s'^2 \mu_0}{2\pi\rho c} \int_{\xi}^{0} d\xi' \, e^{-k_0(\xi'+r')} \left[1 - \frac{\xi'}{r'}\right] \frac{1}{r'} \,, \tag{29}$$

where $r' = \sqrt{\xi'^2 + y^2}$. We have changed variable of integration in Eq. (27) from t' to $\xi' = x - x_0(t')$, with $x_0(t) = vt$, and we have let $I' = I_s'$, where the subscript s indicates that this is the current per height through a sheet. The upper limit of zero comes from the fact that there is very little current ahead of the armature, so a point begins to receive heat essentially only after the armature passes it, for $t' > t_x$, or $\xi < 0$. For the domain where the current has been passing for a time, that is, for $\xi < 0$ and $|k_0 \xi| \gg 1$, with y fixed and small, the integral can be approximated still further. As ξ' varies over its domain, the quantity $\xi' + r'$ stays nearly equal to zero, and all the exponentials are then equal to one. Deviation from this approximation occurs only in the neighborhood of $\xi' = 0$. The integrand can now be approximated by replacing the exponential with a step function.

The resulting integral is then

$$T \approx \frac{I'^2 \mu_0}{\pi \rho c} \int_{\xi}^{0} \frac{d\xi'}{\sqrt{y_1^2 + \xi'^2}}.$$

This is easily evaluated to be

$$T \approx -\frac{I_s'^2 \mu_0}{\pi \rho c} \sinh^{-1}\left(\frac{\xi}{y}\right) \approx \frac{I_s'^2 \mu_0}{\pi \rho c} \ln\left(-2\frac{\xi}{y}\right). \tag{30}$$

From Eq. (30) we see that the isotherm with temperature T_m is the straight line with equation

$$\left|\frac{y}{\xi}\right| = \frac{1}{2} \exp\left[-\frac{\pi \rho c}{\mu_0 I_s'^2} T_m\right]. \tag{31}$$

For copper, the coefficient in this expression is about

$$\frac{\mu_0}{\pi \rho c} = 1.1 \times 10^{-13}\ ^\circ\mathrm{Cm}^2/\mathrm{Amp}^2.$$

The remarkably simple expression in equation (31) has several interesting consequences. The amount of surface melting can be estimated from it if we neglect the latent heat of melting. If the temperature T_m is set equal to the melting point of the rail, we can find the depth to which a given current sheet will melt the surface. For copper, and a current sheet $I_s' = 300{,}000$ Amps/cm of rail height, the slope, $|y/x|$, of the melting curve is found to be 3.0×10^{-5}. The mass of material melted will then be

$$m = \frac{1}{4} \rho R^2 h \exp\left[\frac{\pi \rho c}{\mu_0 I_s'^2} T_m\right], \tag{32}$$

where ρ is the density, R is the length of the rail, and h is the rail height. The exponential dependence of the melted mass, m, on the rail parameters should be noted. Taking $I_s' = 300{,}000$ Amps/cm, $\rho = 8.9$ gm/cm^3, $R = 400$ cm, $h = 1$ cm, and $T_m = 1{,}083\ ^\circ$C, we obtain $m = 5.2$ grams for copper rails. The large amount of melting is due, of course, to the large value used for the current sheet.

Conclusion

The calculations above have been done for an idealized geometry where there are no variations in the z direction. These simplifications were introduced in order to be able to treat the time dependent problem analytically. The formulas obtained, however, should be of value in understanding the performance of railguns. We believe that despite the simplifications, reasonable estimates of rail currents and temperatures can be made using our methods.

We emphasize one of the most interesting results of this paper. This is the possibility of local current density reversals when dI'/dt becomes negative. This is simply an inductance effect. The current reverses direction to try to prevent a decrease in the value of $B_z(x, y, t)$

in the rail. The same reversal can occur in parts of the armature in a real case. The reversal in the armature does not occur in our model because we assume a known current density distribution in the armature and rigorously compute the current in the rails. In the real problem the current distribution in the armature is not specified; only the total current is. Then a decrease in the total current would decrease the magnetic field in the interior of the armature. The current density in the rear of the armature could easily reverse then, just as it did near the rail edge in Fig. 2, in order to try to keep up the value of the magnetic field in the interior of the armature. The portion of the armature where the current is reversed could then be subject to a magnetic force directed toward the breech. This would have a powerfully disruptive effect in the case of a plasma armature.

References

[1] J. F. Kerrisk, "Electrical and Thermal Modeling of Railguns", IEEE Trans. Mag. **MAG-20**, 399 (1984).

[2] J. F. Kerrisk, "Current Diffusion in Rail-Gun Conductors", Los Alamos National Laboratory Report LA-9401-MS (June 1982).

[3] R. A. Marshall, "Current Flow Patterns in Railgun Rails", IEEE Trans. Mag. **MAG-20**, 243 (1984).

[4] G. C. Long, "Railgun Current Density Distributions", IEEE Trans. Mag. **MAG-22**, 1597 (1986).

[5] P.A. Drake, and C. E. Rathmann, "Two-Dimensional Current Diffusion in an EML Rail with Constant Properties", IEEE Trans. Mag. **MAG-22**, 1448 (1986).

[6] H. Knoepfel, "Pulsed High Magnetic Fields", American Elsevier, New York, 1970.

[7] I. S. Gradshteyn and I. M. Ryzhik, Table of Integrals Series and Products, Academic Press, New York, 1980, equation 3.954.2.

[8] *ibid.* equation 8.451.6.

TWO DIMENSIONAL TIME DEPENDENT MHD SIMULATION OF PLASMA ARMATURES

M. A. Huerta and G. C. Boynton
University of Miami
Physics Department
Coral Gables, FL 33124

Abstract

We report on our development of a two dimensional MHD code to simulate internal motions in a railgun plasma armature. We use the equations of resistive MHD, with Ohmic heating, and radiation heat transport. We use a Flux Corrected Transport code to advance all quantities in time. Preliminary runs show the growth and subsequent shedding of vortex structures in response to a small perturbation upon an initial equilibrium.*

Introduction

In a railgun the armature carries the current across from one rail to the other and is subjected to a powerful $\mathbf{J} \times \mathbf{B}$ magnetic force that pushes it against the rear of a projectile. In many cases the strong heat produced by the current generates a plasma armature. The plasma armature is then a hot, high density, high pressure arc undergoing rapid acceleration. The magnetic force compresses the plasma and causes a high pressure at the front, where the plasma pushes against the projectile. The pressure takes a profile that diminishes toward the rear as the plasma approaches a region of much lower pressure and density .

Much of the modeling of plasma armatures in railguns begins with the one and two dimensional, infinite rail height, MHD models of Powell and Batteh[1,2]. Their models describe a great deal of the physics, including radiation transport, and the degree of plasma ionization. Those models assume that the plasma is in a steady state with no flow in the frame of the accelerating armature, and yield profiles of the magnetic field, and of the fluid properties in the armature. Some work has been reported by Sloan[3] on extending the steady models to three dimensions.

The steady state assumption is an important limitation of those models. The calculations of Huerta and Decker[4,5], as well as those of Powell[6], give that the steady plasma armature is subject to the MHD flute instability that occurs when a magnetic field accelerates a plasma. The flute instability causes two dimensional corrugations of the rear of the plasma that, together with ensuing flows, may destroy the simple steady states found by the methods of Refs. [1]–[3]. Recently[7,8], studies have been reported on one dimensional time dependent models. These numerical studies emphasize armature initiation phenomena, and are not able to assess the effects of two dimensional instabilities on the overall steady state.

We report our work on a two dimensional, MHD, infinitely tall rail, time dependent numerical simulation of the behavior of the plasma armature. Our model is capable of describing not only the growth of the flute instability, but also other two dimensional

* This work supported in part by the Air Force Office of Scientific Research under grant number 84-0116.

effects, such as the shedding of plasma at the rear of the arc, and convective transport in the armature. We also seek to describe current filamentation, possible current reversal due to a drop in total current, armature disruption due to the rearward forces on the reversed currents, as well as a variety of waves, and shocks.

The numerical solution of the governing two dimensional MHD equations is accomplished with an algorithm which is designed to take advantage of the architecture of Multi-Vector processor supercomputers.The basic algorithm for advancing the critical quantities in time is a finite difference, explicit, Eulerian, Flux Corrected Transport (FCT) sub-code which closely follows an algorithm developed at NRL[9,10].

The Governing MHD Equations

The plasma is collision dominated and can be described by the equations of magnetohydrodynamics subject to the usual limitations of MHD[11]. The plasma is treated as a single fluid of density ρ, velocity $\mathbf{v}$, pressure p, energy per unit mass e, and temperature T. We choose the x–axis along the rail direction, from the projectile back toward the breech, and the y–axis is transverse to it, opposite to the direction of the current in the armature, with the z axis along the direction of the magnetic field between the rails. The projectile moves relative to the rails with a velocity v_p toward the muzzle. Our coordinate system is fixed to the projectile. When we speak of the fluid velocity $\mathbf{v}$, the electric field $\mathbf{E}$, or any other quantity, we mean it as measured in the frame of reference that moves with the armature, unless otherwise specified. It is easy to show that the only relevant ($v_p \ll c$) change in the fluid and Maxwell equations brought about by our choice of moving coordinate system, is the appearance of a "gravity term $\mathbf{g}$" in the momentum equation, where

$$\mathbf{g} = g\hat{\mathbf{x}} = \frac{dv_p}{dt}\hat{\mathbf{x}}. \qquad (1)_0$$

Therefore, as the armature gains speed toward the muzzle, $g = dv_p/dt > 0$,and $\mathbf{g}$ points toward the breech. All quantities are taken independent of z in our two dimensional model (translational invariance along the z axis, $0 = \partial/\partial z$ as for infinitely tall rails). The magnetic field only has a z component, but the fluid velocity, and the current do not have z components.

In MHD the relevant Maxwell equations are

$$\nabla \cdot \mathbf{B} = 0, \quad \nabla \times \mathbf{E} = -\frac{\partial \mathbf{B}}{\partial t}\ , \qquad (2)_1$$

and

$$\nabla \times \mathbf{B} = \mu_0 \mathbf{J}\ . \qquad (3)_2$$

The displacement current has been neglected in Ampere's law, Eq. (3), because only frequencies much lower than σ/ϵ_0 are considered. The electric field is given by a simple Ohm's law

$$\mathbf{J} = \sigma(\mathbf{E} + \mathbf{v} \times \mathbf{B}), \qquad (4)_3$$

where σ is usually taken as the Spitzer conductivity[1]. Solving Eq. (4) for $\mathbf{E}$, eliminating $\mathbf{J}$ using Eq. (3) and substituting into Eq. (2) one obtains the equation that advances $\mathbf{B}$ in

time

$$\frac{\partial B_z}{\partial t} + \nabla \cdot (B_z \mathbf{v}) = \frac{\partial}{\partial x}\left[\frac{1}{\mu_0 \sigma}\frac{\partial B_z}{\partial x}\right] + \frac{\partial}{\partial y}\left[\frac{1}{\mu_0 \sigma}\frac{\partial B_z}{\partial y}\right]. \quad (5)_4$$

The quantity $1/\mu_0\sigma$ inEq. (5) is a coefficient of magnetic diffusion. When the magnetic diffusion coefficient is small (large σ), the magnetic field tends not to diffuse, but rather to be convected along with the fluid. When the diffusion coefficient is large, the magnetic field diffuses through the conducting fluid. The tall rails carry a current I' per unit height. A real rail of height h carrying a current I is modelled by a current

$$I' = \frac{I}{h}. \quad (6)_{4a}$$

In the space behind the armature, where there is no current, the magnetic field is uniform with the value

$$B_z(t) = \mu_0 I'(t). \quad (7)_{4b}$$

In MHD the plasma is treated as a single conducting fluid even though it consists of several fluids. The inertia is carried essentially by the heavy particles. The electron fluid is not treated explicitly but has its effect via the current $\mathbf{J}$. The fluid equations are the usual ones. First the equation of mass conservation

$$\frac{\partial \rho}{\partial t} + \nabla \cdot (\rho \mathbf{v}) = 0, \quad (8)_5$$

which advances ρ in time. The fluid velocities v_x and v_y are advanced by the equations for the x and y components of momentum,

$$\frac{\partial(\rho v_x)}{\partial t} + \nabla \cdot (\rho v_x \mathbf{v}) = -\frac{\partial}{\partial x}(p + \frac{1}{2\mu_0}B_z^2) + \rho\frac{dv_p}{dt}, \quad (9)_6$$

and

$$\frac{\partial(\rho v_y)}{\partial t} + \nabla \cdot (\rho v_y \mathbf{v}) = -\frac{\partial}{\partial y}(p + \frac{1}{2\mu_0}B_z^2). \quad (10)_7$$

In Eqs. (9) and (10), the magnetic force $\mathbf{J} \times \mathbf{B}$ has been rewritten by eliminating $\mathbf{J}$ as usual from Eq. (3). This makes the magnetic force appear as the gradient of a magnetic pressure $B_z^2/2\mu_0$. The fluid pressure p is advanced from the equation for the energy e per unit mass,

$$\frac{\partial(\rho e)}{\partial t} + \nabla \cdot (\rho e \mathbf{v}) + p\nabla \cdot \mathbf{v} = -\nabla \cdot \mathbf{q} + \frac{J_x^2}{\sigma} + \frac{J_y^2}{\sigma}, \quad (11)_8$$

and relating p to e using an energy equation. The simplest energy equation is for the monoatomic ideal gas with $\gamma = 5/3$,

$$e = (\gamma - 1)p/\rho\ . \quad (12)_9$$

There are several effects, such as variations in the degree of ionization,that require modification of Eq. (12). The temperature T is introduced via an equation of state. One of the simplest[1] is for an ideal gas of ions and electrons

$$p = (1 + \alpha)\rho k_B T/m_0, \quad (13)_{10}$$

where α, the ratio of electrons to heavy particles, is discussed in Ref. [1], and m_0 is the mass of the ion or neutral particle. The current dependent terms in the right hand side of Eq. (11) represent Ohmic heating. The term with the heat flow vector $\mathbf{q}$, represents heat transfer. The form of $\mathbf{q}$ in terms of T for radiation transport in the diffusion approximation is given in Ref. [1].

Boundary conditions

The front boundary of the plasma, at $x = 0$ is up against the back of the projectile. The plasma pressure acting over the rear area of the projectile provides the force that pushes the projectile forward and must satisfy the boundary condition

$$\int_0^w p(x = 0, y, t)\, h\, dy = m_p \frac{dv_p}{dt}, \qquad (14)_{10a}$$

where w is the rail separation.

We have placed a low density region of zero conductivity inside the region of computation at the rear of the plasma. The conductivity is set to zero when the density falls below a certain threshold value which we take approximately five hundred times less than the density near the projectile. This boundary between a region of conductivity and a region of no conductivity has to be treated carefully since it is not a fixed boundary. In the region of no current the fluid properties are still calculated and advanced in time from the fluid equations. The magnetic field, however, is simply uniform in the rear $\mathbf{J} = 0$ region, and given by Eq. (7). As soon as the density at a cell rises above the threshold density for conductivity, its properties are advanced with the full set of MHD equations.

The rails are treated as infinitely conducting. We take the boundary condition that the tangential electric field in the frame of the rails is zero. This forces the normal derivative of the magnetic field, $\partial B_z/\partial y$ to be zero at the rail surfaces. The value of $\partial B_z/\partial y$ at the rails is needed in the right hand side of Eq. (5), because of the second derivative with respect to y, to advance B_z at the center of a cell adjacent to a rail. At the rear of the projectile we have $J_x = 0$, which sets $B_z =$ constant, in fact zero, along the $x = 0$ boundary. This enables us to calculate the second derivative of B_z with respect to x at a cell adjacent to the projectile. The other boundary conditions are standard except for the heat flow vector at the boundaries of the plasma. Here, in order to evaluate $\nabla \cdot \mathbf{q}$ in the right hand side of Eq. (11) we need the normal component of $\mathbf{q}$ at each boundary. Physically we need a statement of how the plasma radiates to its surroundings. A variety of conditions are possible, such as the one used in Ref. [1],

$$q_n = 2\sigma_s T_b^4 \qquad (15)_{11}$$

where q_n is the component of $\mathbf{q}$ along the outward normal at the plasma boundary, and T_b is the plasma temperature at the boundary. The factor of 2 in Eq. (15) is explained by Zeldovich[12]. The radiation that leaves the plasma actually comes from some distance in its interior, where the temperature is a bit higher than at the surface, $2^{1/4}$ higher.

Numerical Methods

We do a two dimensional, Eulerian calculation using a fixed rectangular array of square cells. A typical grid will have 20 cells in the y direction to cover the one cm rail separation, and 240 cells in the x direction. The main conducting plasma, which initially is set at 10 cm length, extends from cell 1 to 200. Beyond cell 200 we have a low density, nonconducting gas region that extends to the end of the computational region at cell 240. As the flows develop, any gas on a cell in the 240^{th} row, with a velocity to the rear, is allowed to escape.

The time integration uses a simple midpoint rule which is second order accurate. The driving variables are determined at the half step by a forward differenced first-order algorithm, and are then used to advance all the variables a full time step in a time centered manner. We use a one dimensional FCT[9,10] code that is optimized for a vector processor. In order to preserve the optimization we do the two dimensional problem with the one dimensional FCT, and a time step splitting technique[13]. The time step splitting technique can also take advantage of the capabilities of multi-processor machines.

This FCT is an explicit, finite difference technique that is essentially second order accurate, and has strict limits on its stability. It imposes, however, the further conditions that densities, such as ρ, and e remain positive. This makes it of indeterminate order, but enables it to yield physically realistic and accurate results, even in the presence of inviscid shocks and steep gradients. The algorithm provides fourth order accurate phases and minimum residual diffusion. It consists conceptually of two stages. The usual transport stage is followed by a corrective antidiffusive stage. FCT has been used by Emery[14], for example, in the study of Rayleigh-Taylor instabilities on the surface of targets accelerated by laser ablation.

Results

The code is optimized to run on a supercomputer with vector processing, but so far we have only run preliminary tests on a VAX 8650, where it runs rather slowly. With a grid of 20×240 cells, it advances some 1,000 time steps in about one hour of CPU time.

We report preliminary results. We have set up programs to do simulations with parameters similar to Ref. [1]. A typical case has a plasma of copper ions, $m_0 = 1.1 \times 10^{-25}$ kg, with a projectile mass of $m_p = 2$ gm, and a plasma mass of .065 gm. The railgun cross section has $h = 1$ cm, and $w = 1$ cm. The preliminary runs have an adiabatic energy equation (zero right hand side in Eq. (11)), and all the atoms doubly ionized, with degrees of ionization $x_1 = 0, x_2 = 1$, as defined in Ref. [1]. For the current per unit height we take $I' = 2 \times 10^7$ Amp/m. This produces a magnetic field of 8π T from Eq. (7). The pressure on the projectile is of the order of 2,500 atmospheres and the projectile acceleration is of the order of 1.2×10^7 m/sec^2. The preliminary runs have a constant conductivity $\sigma = 1 \times 10^5$ (ohm-m)$^{-1}$, that is turned off to zero where the plasma density falls below 2.61×10^{-2}kg/m^2 at the plasma rear. The linear growth rate of the flute, or interchange instability, is about

$$\gamma = \sqrt{kg} = \sqrt{\frac{2\pi g}{\lambda}}. \qquad (16)_{12}$$

Eq. (16) is the same[4,6] as the Rayleigh-Taylor, or Kruskal-Schwarzschild rate. According to this, we expect the interchange instability to develop with a growth rate of 8.6×10^4

$\sec^{-1}$ in this example.

The grid has 240 cells along the x axis. At $t = 0$ we set up a plasma equilibrium that, except for the temperature, is pretty much as calculated in Ref. [1]. The plasma is 10 cm long and extends to cell 200. The initial temperature is made uniform and set at 6.72×10^4 K. The plasma is initially at rest in the frame of the projectile except for a velocity perturbation of 10 m/s in v_x from cell 199 to 201. The velocity perturbation varies sinusoidally in y with a wavelength of 2/3 cm or about 13 y-cells. The v_x perturbation is set positive (rearward) near the walls, and negative near the center. In the same cells we also perturb the pressure by 2% of its local equilibrium value with the same variation in y as the velocity perturbation. We also perturb the pressure, again by 2% of its local equilibrium value, in the interior of the plasma, corresponding to cells 99-101.

We find that the calculation is numerically unstable for time steps longer than about $\Delta t = 2 \times 10^{-9}$sec. This is as expected from the Courant[15] condition, $|v|\Delta t \leq \Delta x$, due to the large local velocities produced in the low density region. To simulate a shot down a one meter long barrel requires a flight time of about 0.4×10^{-3} sec. This amounts to some 2×10^5 time steps. In the VAX 8650 this would amount to some 200 hours of CPU time.

We show the results of a run that used $\Delta t = 1.86 \times 10^{-9}$ sec, and went for 40,500 steps, a total time $T = 7.5 \times 10^{-5}$ sec, and required about 40 hours of CPU time on the VAX 8650. According to the linear growth rate of Eq. (16), the perturbation should grow by $e^{\gamma T} \approx e^{6.4}$. Fig. 1 shows the pressure profile at $t = 0$. The initial 2% perturbation is practically invisible in the profile.

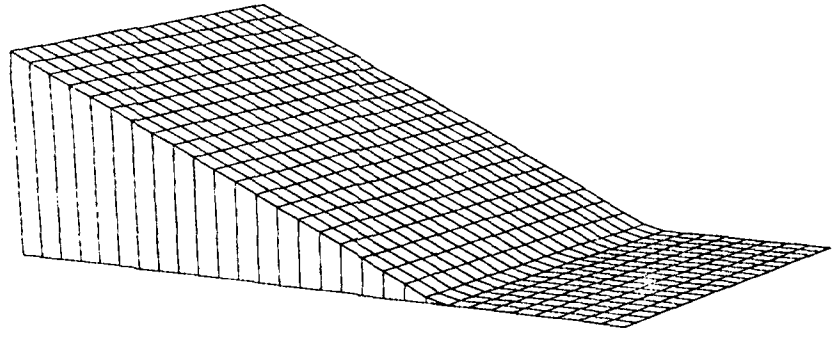

Fig. 1. Pressure profile at t=0, s=0, cells 180–210.

Fig. 2 shows the current **J** after 7,000 time steps, $t = 13 \times 10^{-6}$sec, distance travelled $s = 1.0 \times 10^{-3}$m, projectile velocity $v_p = 1.6 \times 10^2$m/sec and projectile acceleration $a_p = 1.22 \times 10^7$m/sec^2. It shows that the conducting boundary has oscillated, and a dominant mode is developing.

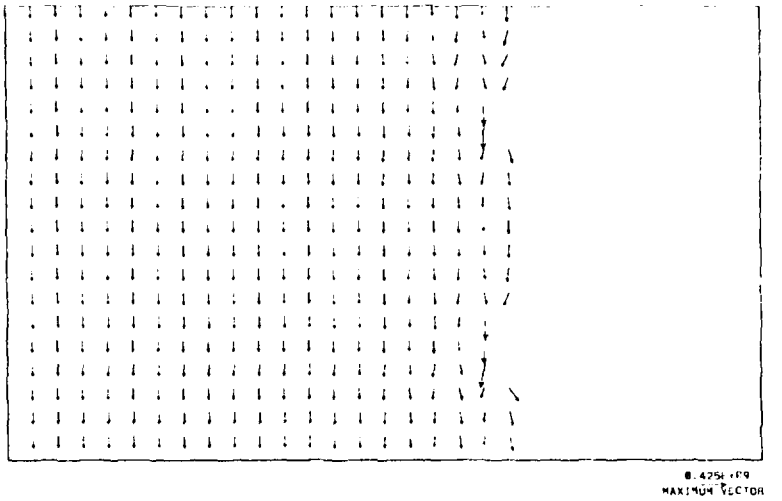

Fig. 2. **J** at 7,000 steps, $t = 13 \times 10^{-6}$ sec, $s = 1.0 \times 10^{-3}$m, cells 180–210.

Fig. 3 shows the pressure profile after 17,500 time steps, $t = 3.3 \times 10^{-5}$sec, $s = 6.5 \times 10^{-3}$m, $v_p = 4.0 \times 10^2$m/sec and $a_p = 1.22 \times 10^7$m/sec^2. It has a noticeable bulge.

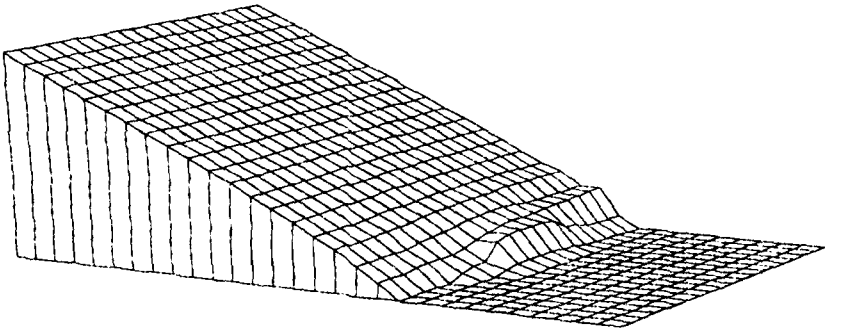

Fig. 3. Pressure profile at $t = 3.3 \times 10^{-5}$sec, $s = 6.5 \times 10^{-3}$m, cells 180–210.

Fig. 4 shows the pressure profile after 27,000 time steps, $t = 5.0 \times 10^{-5}$sec, $s = 1.5 \times 10^{-2}$m, $v_p = 6.1 \times 10^2$m/sec and $a_p = 1.22 \times 10^7$m/sec^2.

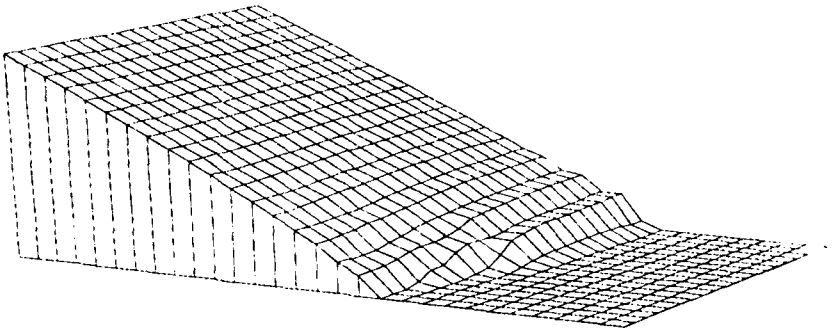

Fig. 4. Pressure profile at $t = 5.0 \times 10^{-5}$sec, $s = 1.5 \times 10^{-2}$m, cells 180–210.

Fig. 5 shows the current also after 27,000 time steps. It shows further boundary deformation.

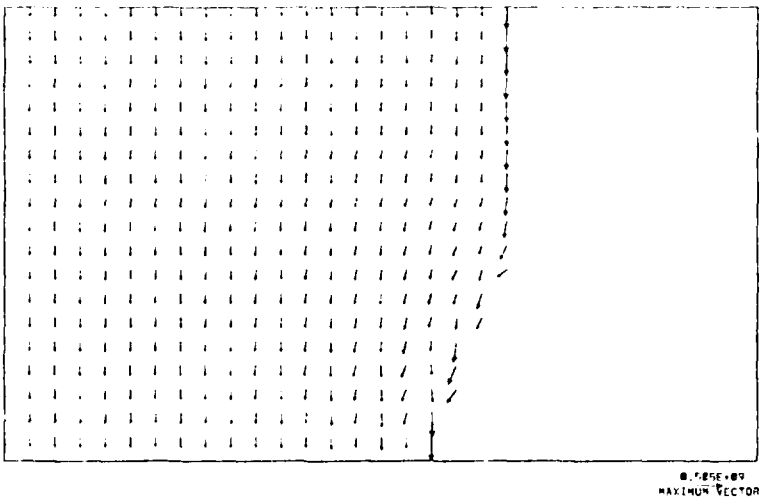

Fig. 5. **J** at 27,000 steps, $t = 5 \times 10^{-5}$ sec, $s = 1.5 \times 10^{-2}$m, cells 180–210.

Fig. 6 shows the velocity field v also after 27,000 time steps, from cells 160–190, not quite to the end of the conducting region. It corresponds to the pressure profile of Fig. 4.

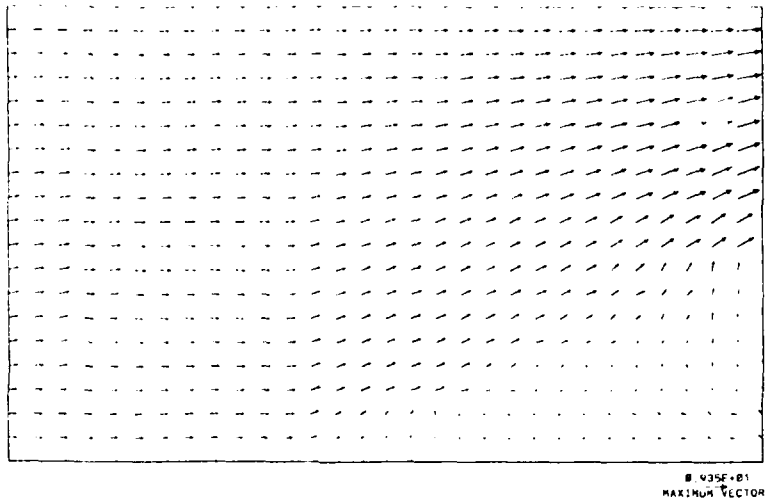

Fig. 6. $\mathbf{v}$ at $t = 5.0 \times 10^{-5}$sec, $s = 1.5 \times 10^{-2}$m, cells 160–190.

Fig. 7 shows the pressure profile after 40,500 time steps, $t = 7.5 \times 10^{-5}$sec, $s = 3.5 \times 10^{-2}$m, $v_p = 9.2 \times 10^2$m/sec and $a_p = 1.22 \times 10^7$m/sec^2.

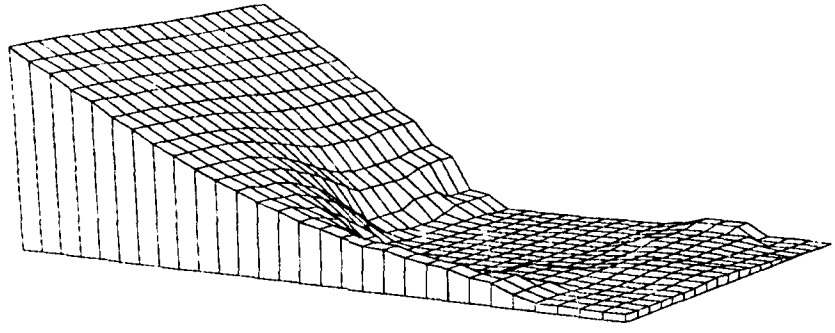

Fig. 7. Pressure profile at $t = 7.5 \times 10^{-5}$sec, $s = 3.5 \times 10^{-2}$m, cells 185–215.

Fig. 8 shows the current also after 40,500 time steps. It shows that the boundary deformation is beginning to get important. Even though the armature has travelled only 3.5 cm, there is already a bit of plasma shed at the rear. The linear growth rate gets larger for the shorter wavelength modes. However, they do not appear to grow to large amplitudes. This is due to nonlinear saturation effects, as also found by Emery[14].

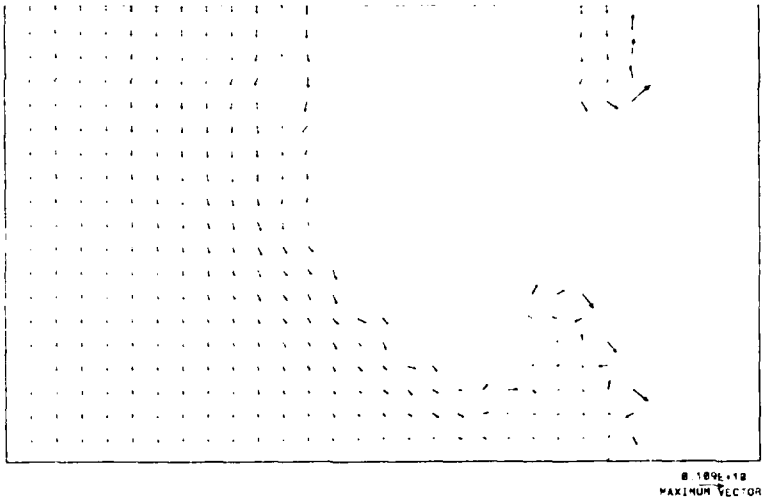

Fig. 8. **J** at $t = 7.5 \times 10^{-5}$sec, $s = 3.5 \times 10^{-2}$m, cells 185–215.

References

1. Powell, J. D., and Batteh, J. H., "Plasma Dynamics of an Arc-Driven Electromagnetic Projectile Accelerator," J. Appl. Phys., **52**, 2717 (1981)
2. Powell, J. D., and Batteh, J. H., "Two Dimensional Plasma Model for the Arc Driven Rail Gun," J. Appl. Phys., **54**, 2242 (1983).
3. Sloan, M. L., "Physics of Rail Gun Plasma Armatures," IEEE Trans. Mag., **MAG-22**, 1747 (1986).
4. Huerta, M. A., and Decker, A. M., "Plasma Armatures and the MHD Exchange Instability," 1985 IEEE International Conference on Plasma Science, Pittsburgh, Pennsylvania, June 3–5, 1985.
5. Decker, A. M., "Finite Conductivity and the Rayleigh-Taylor Interchange Instability, with Applications to Plasma Arcs in Electromagnetic Rail–Launch Devices," Ph. D. dissertation, June, 1986. Physics Department, University of Miami, coral Gables, Florida 33124.
6. Powell, J. D. "Interchange instability in railgun arcs," Phys. Rev. A **34**, 3262 (1986).
7. Powell, J. D., and Jamison, K. A., "One Dimensional Time Dependent Model for Railgun Arcs," U. S. Army Ballistic Research Laboratory, Technical Report No. BRL-TR-2779, February, 1987.
8. Batteh, J. H., and Rolader, G. E., "Modeling of Transient Effects in Railgun Plasma Armatures," U. S. Army Ballistic Research Laboratory, Contract Report No. BRL-CR-567, March 1987.
9. Boris, J. P., and Book, D. L., Methods Comput. Phys. **16** 85 (1976).
10. Boris, J. P., et al "Finite–Difference Techniques for Vectorized Fluid Dynamics Calculations," Springer–Verlag, New York, 1981.
11. Kulsrud, R. M., "MHD description of plasma," p.115 in "Handbook of Plasma Physics'" Vol. 1, edited by M. N. Rosenbluth, and R. Z. Sagdeev, North Holland Publishing Company, New York, 1983.

12. Zeldovich, Y. B., and Raizer, Y. P., "Physics of Shock Waves and High-Temperature Hydrodynamic Phenomena," Academic Press, New York, 1966.
13. Book, D. L., Boris, J. P., and Hain, K., "Flux-Corrected Transport II: Generalizations of the Method," J. Comp. Phys. **18** 248 (1975).
14. Emery, M. H., Gardner, J. H., and Boris, J. P., "Vortex shedding due to laser ablation," Phys. Fluids **27**, 1338 (1984).
15. W. H. Press, Flannery, B. P., Teukolsky, S. A., and Vetterling, W. T., "Numerical Recipes, The Art of Scientific Computing," Cambridge University Press, New York, 1986.

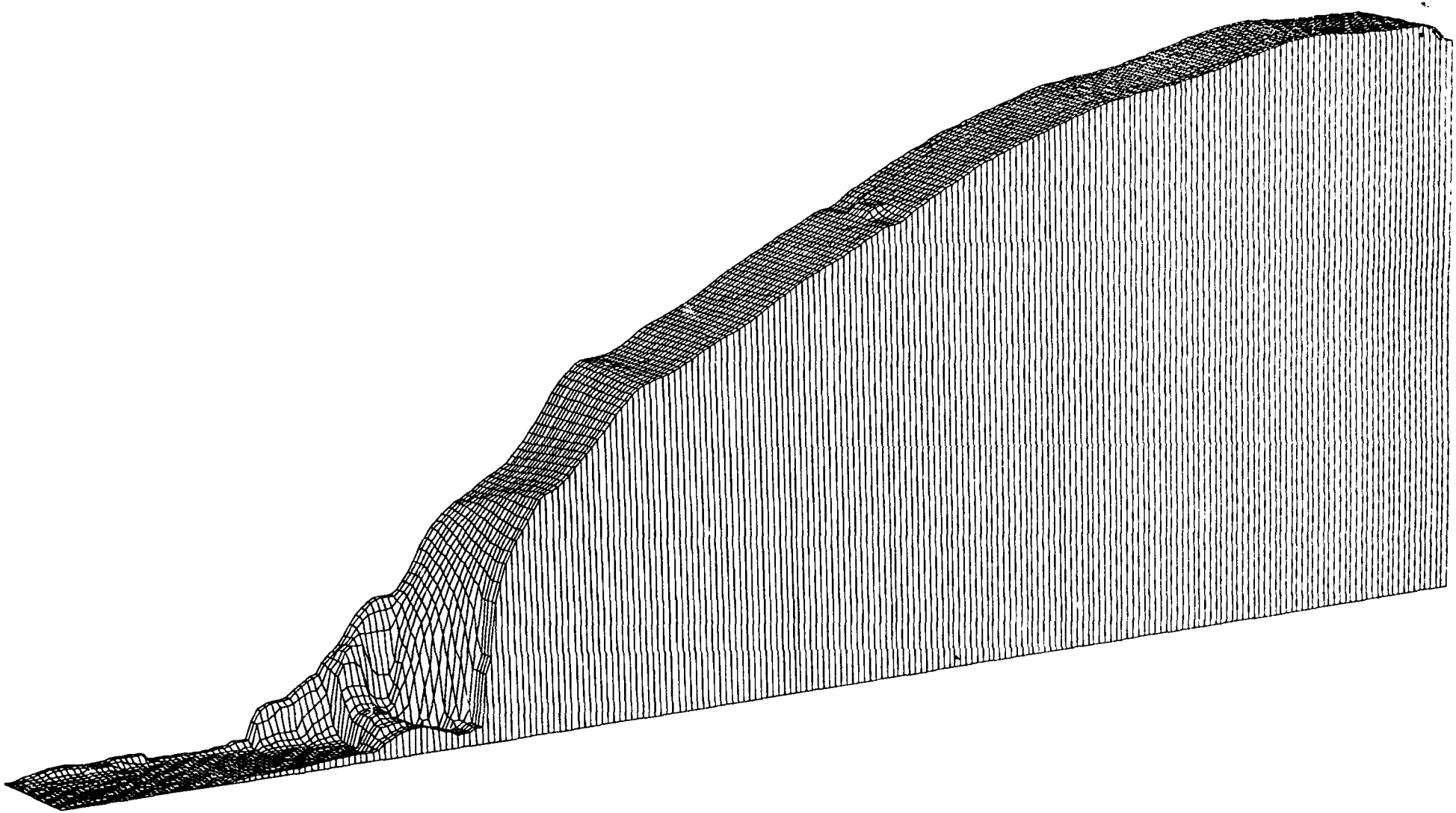

Time = 8.7E-05 s, SFRM = 4.6E-02 m, VFRM = 1.1E+03 m/s, AFRM = 1.20E+07 m/s^2
Projectile toward right

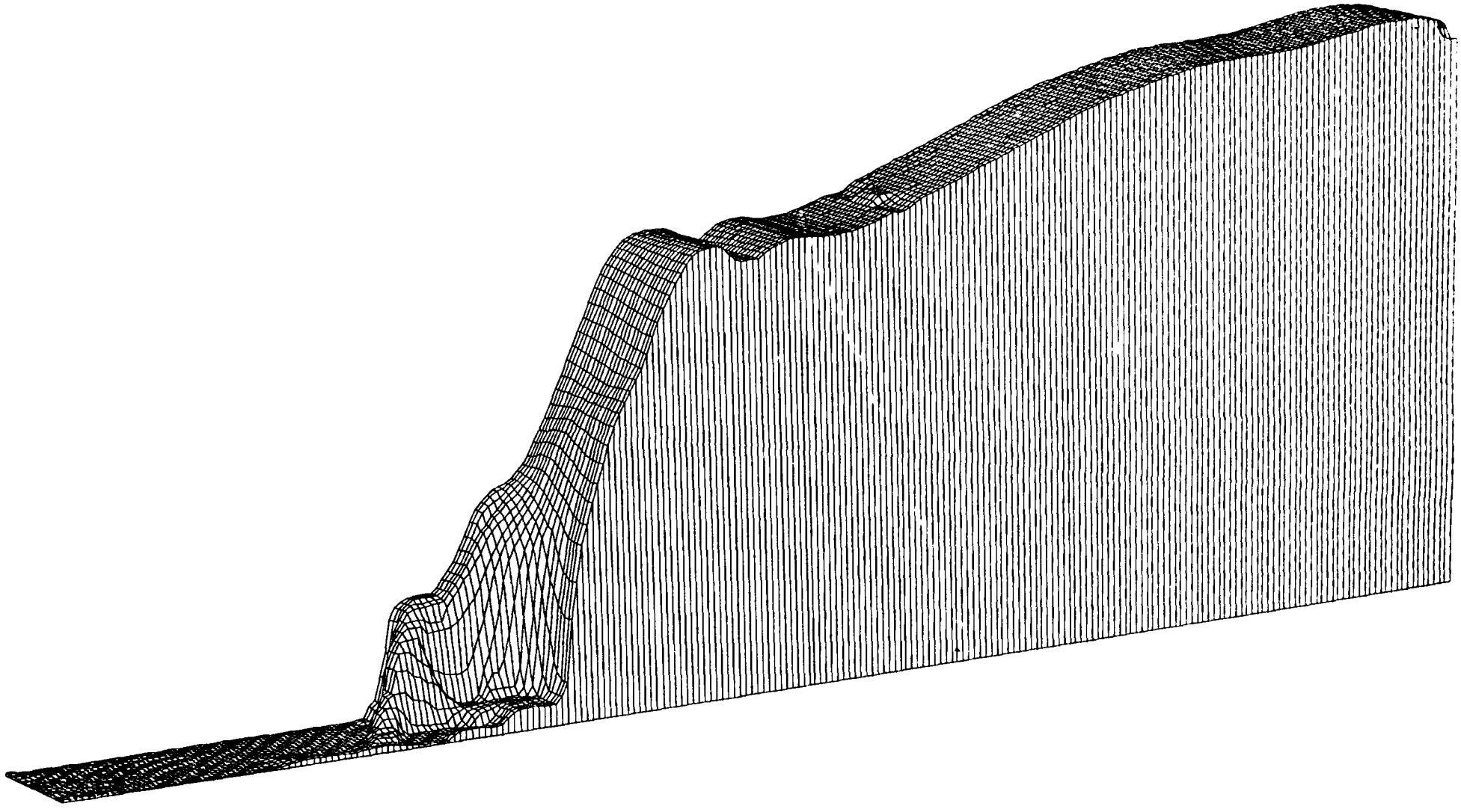

Time = 8.8E-05 s, SFRM = 4.7E-02 m, VFRM = 1.1E+03 m/s, AFRM = 1.22E+07 m/s^2
Projectile toward right

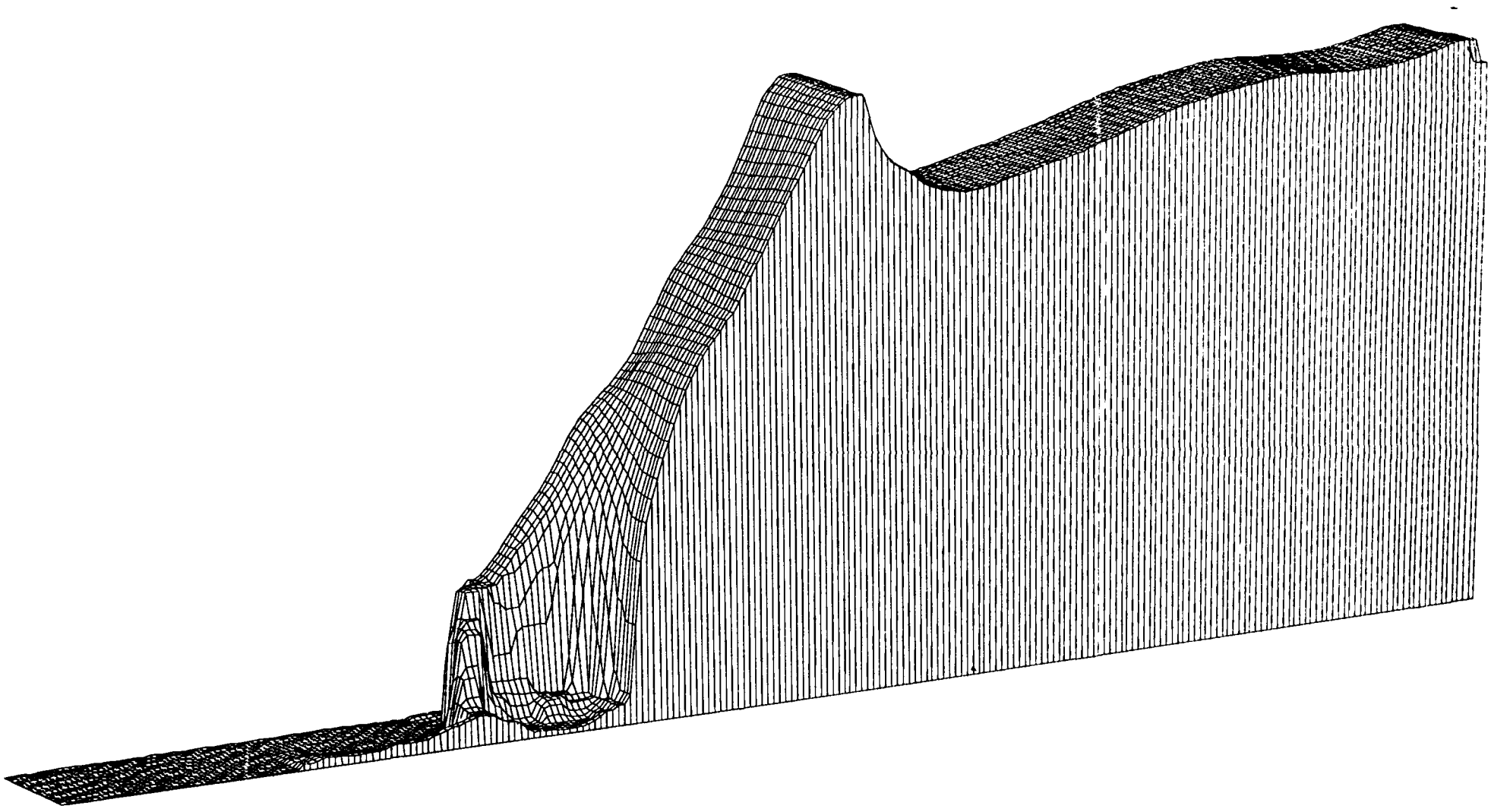

Time = 8.9E-05 s, SFRM = 4.8E-02 m, VFRM = 1.1E+03 m/s, AFRM = 1.26E+07 m/s^2
Projectile toward right

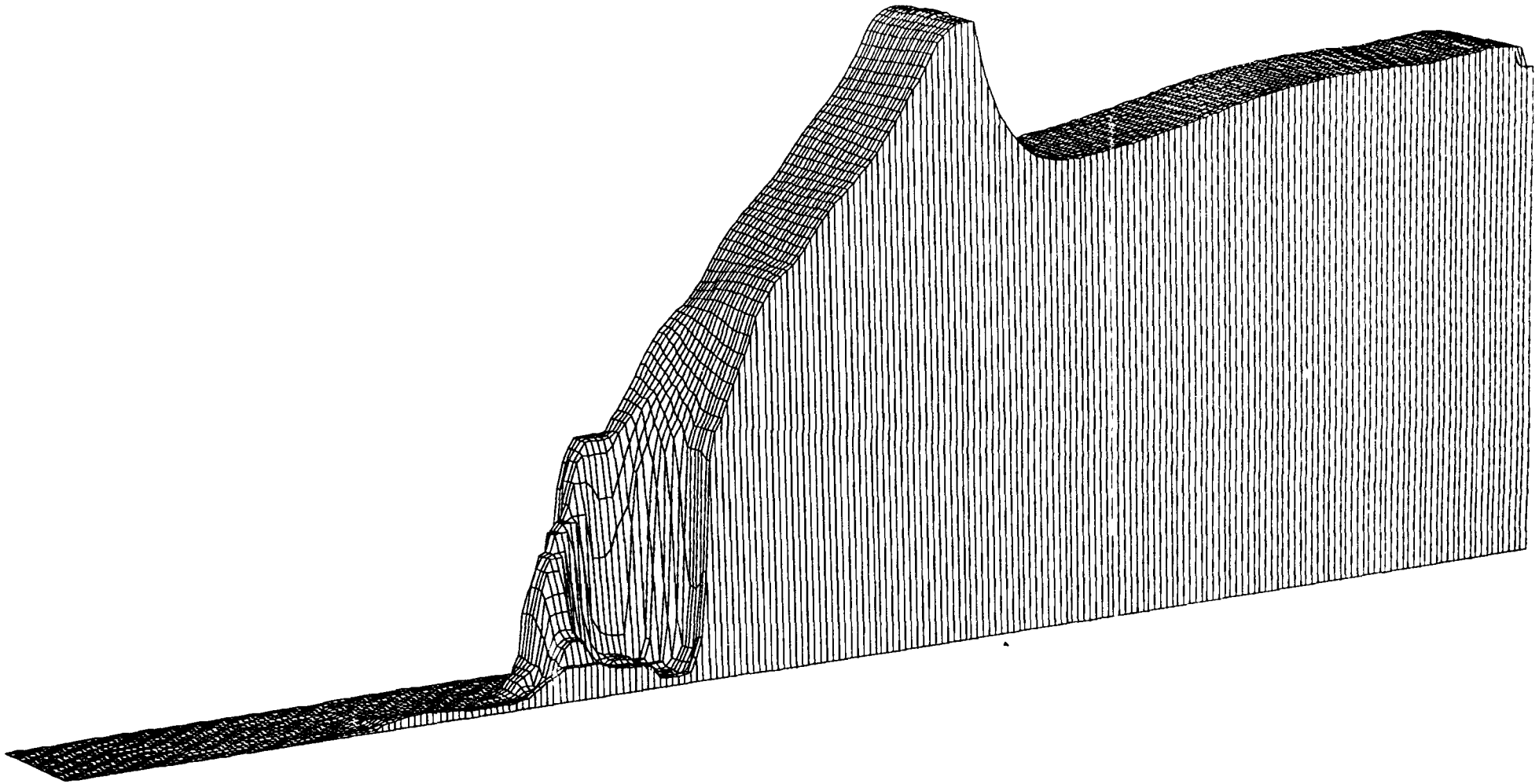

Time = 8.9582E-05 s, SFRM = 4.9E-02 m, VFRM = 1.1E+03 m/s, AFRM = 1.24E+07 m/s^2
Projectile toward right

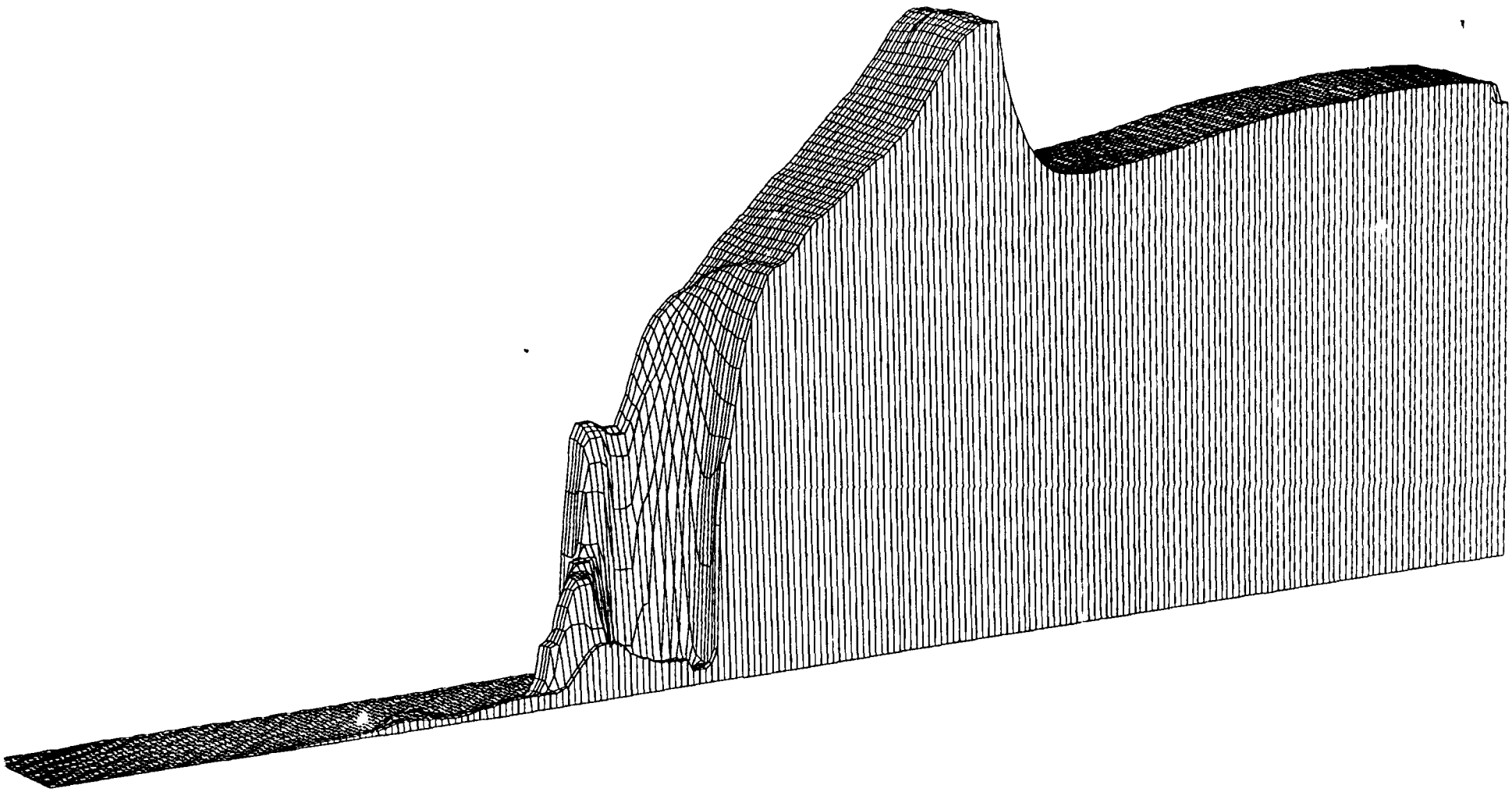

Time = 8.9873E-05 s, SFRM = 4.9E-02 m, VFRM = 1.1E+03 m/s, AFRM = 1.22E+07 m/s^2
Projectile toward right
1_240_rho_200000.psc